A Powerful Tool

Use of Time-Dependent MEQ Tomography for Monitoring Producing Geothermal Reservoirs

G. R. Foulger (University of Durham - Durham, United Kingdom)
and B. R. Julian (U.S. Geological Survey - Menlo Park, CA)

Energy production at geothermal areas causes physical changes in reservoirs through changes of temperature, pressure, and phase of pore fluids and the progressive removal of water. These changes affect seismic wave speeds, which can be detected using time-dependent microearthquake (MEQ) tomography. In this way, MEQs-often regarded as curiosities or nuisance side-effects of production-may be utilized as a powerful reservoir monitoring tool. The method has been applied to study The Geysers, Mammoth Mountain (Long Valley Caldera), and the Coso geothermal area, all in California. The most ambitious study was performed at The Geysers, where tomographic inversions were conducted for suites of MEQs recorded in 1991, 1993, 1994, 1996 and 1998. A strong V_p/V_s anomaly correlates spatially with the producing reservoir. This anomaly became stronger from 1991 to 1998, and delineates a volume where pressure declined, pore water was replaced by steam, and clay minerals were dehydrated. Mammoth Mountain is an active volcano that has been venting carbon dioxide (CO2) at a high rate since 1989. Time-dependent tomography conducted there for 1989 and 1997 reveals an increase in V_p/V_s in a region girdling the volcano. This anomaly growth may indicate the migration of CO2 into the top ~2 km of Mammoth Mountain, accompanied by depletion in peripheral volumes beneath surface venting areas. Preliminary results from time-dependent tomography at the Coso geothermal area suggest an area of decreasing V_p/V_s in the most productive part of the reservoir. Several developments are desirable to optimize time-dependent MEQ tomography, but the method holds the promise of

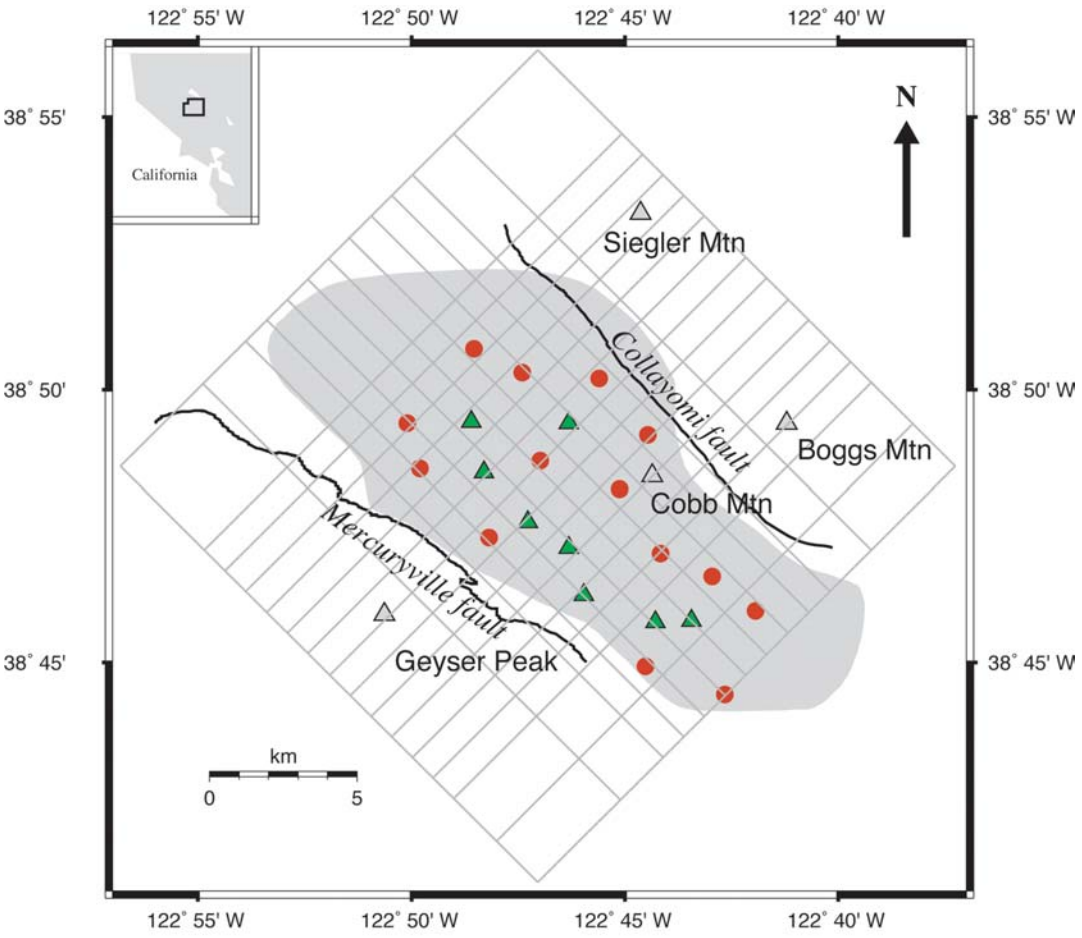

Figure 1 - Map of The Geysers geothermal area. The production area is shaded grey. Red dots: seismometers with vertical sensors only, green triangles: three-component seismometers, grey triangles: geographic features as labeled. The grid shown was used for the tomographic inversions shown in Fig. 2 (adapted from Gunasekera et al., 2003).

Figure 2 - Anomalies in V_p/V_s at The Geysers for sea level (upper panels) and 1.0 km below sea level (lower panels). White line: steam reservoir; red line: felsite batholith that occupies the deeper parts of the reservoir; white triangle: Cobb Mountain; thick black lines: major faults. (a) structure for the year 1991. The contour lines show various measures of quality of the results. The black contour bounds the area within which the spread is < 2 km, the solid orange contour bounds the area within which the resolution is > 0.005, and the dashed orange contour bounds the area within which the standard error is < 0.005. The three-dimensional model is most reliable within these contours. (b) - (e), differences between the 1991 structure and those for 1993, 1994, 1996 and 1998. The leftmost color scale refers to (a) and the rightmost color scale refers to (b) - (e). In peripheral regions, well outside the contours, the starting one-dimensional model is unperturbed and appears as green (adapted from Gupasekera et al., 2003).

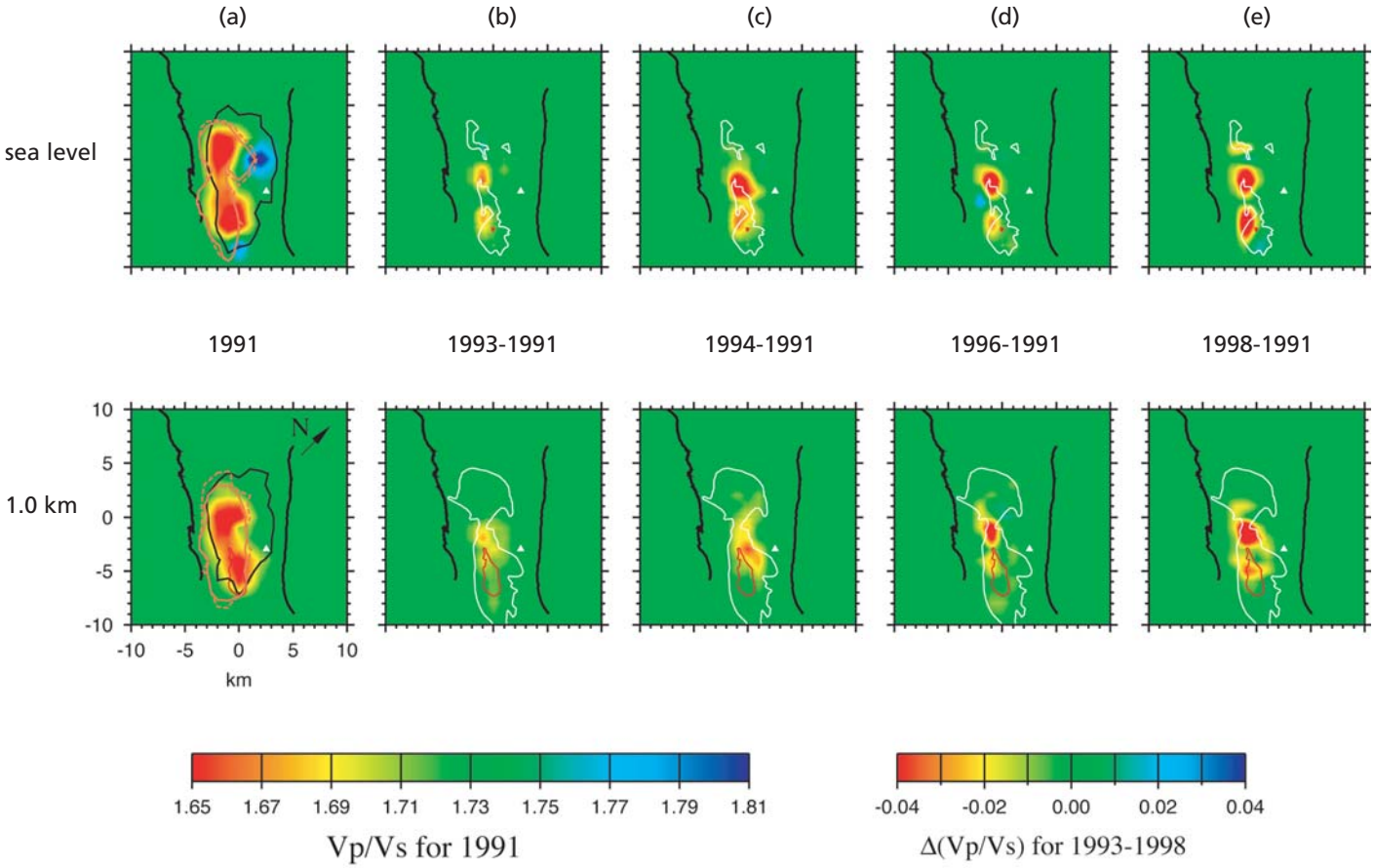

ultimately becoming an important new tool for reservoir-wide monitoring of producing geothermal fields.

Introduction

The removal of fluid from geothermal reservoirs by production, and its reintroduction through injection, can induce changes in the fluid phase, pressure and temperature of the reservoir and in the physical properties of the rock matrix. These changes in turn may affect the seismic properties to a measurable degree, particularly the seismic wave speeds. Reservoirs that produce large amounts of fluid may experience changes that are detectable on a time scale of 1-2 years. Measuring these changes is potentially an effective way of monitoring conditions within exploited geothermal reservoirs.

Processes such as the replacement of pore water by steam, pressure reduction, and the dehydration of hydrous minerals that occur in the rock matrix affect compressional- and shear-wave speeds (V_p and V_s) differently. If both V_p and V_s are monitored the different effects may be separable. Detonating properly situated explosions large enough to provide suitable seismic sources is generally not practical in producing fields, and in any case explosions do not generate strong shear waves. However, production and injection often induce microearthquakes (MEQs), which are ideal seismic sources because many of them occur deep within the reservoir and they generate both shear waves and compressional waves of useful amplitudes.

Time-dependent three-dimensional tomography for V_p and V_s is the most powerful technique for using MEQs to monitor production-related reservoir changes. Depending on the level of production and the seismicity rate, a repeat time of about 2 years is appropriate. MEQ tomography involves iteratively calculating MEQ locations and three-dimensional wave-speed structure from the arrival times of seismic waves at a network seismometers within the study area (Eberhart-Phillips, 1986; Thurber, 1981). Such experiments ideally require the following elements:

- Adequate MEQ activity, *i.e.*, several hundred well-recorded earthquakes per year

well distributed throughout the area of interest, and
- A good seismometer network, preferably digital and including at least 10 three-component stations.

Changes in the data caused by small changes in reservoir structure from year to year are subtle. Thus, it is important to eliminate systematic biases that might camouflage the effects being investigated. The same initial one-dimensional starting crustal model, structural parameterization and seismic-station arrays should be used for different epochs, and the inversion damping values must be chosen for each geothermal field to suppress all but the most robust results. Suitable data-processing strategies for individual field areas must be developed by trial and error in each case.

To date, we have conducted time-dependent tomography studies for The Geysers geothermal area, the active volcano Mammoth Mountain in Long Valley caldera, and at the Coso geothermal area, all in California. In all these studies, we used the local-earthquake tomography program SIMULPS12 (Evans, et al., 1994; Thurber, 1981) and the analysis procedure is described in detail by Foulger, et al. (1995) and Gunasekera, et al. (2003). Experiments in geothermal fields in Indonesia, have also given positive results, but these are not yet publicly released. The use of time-dependent tomography is likely to become standard in modern reservoir monitoring over the next few years.

CASE HISTORIES

The Geysers, California

The Geysers geothermal reservoir occupies greywacke sandstones in the coastal ranges of northern California (Fig. 1). Its surface area is about 75 km2 and it extends from the near surface, at about 1 km above sea level, down to at least 3 km below sea level. The fluid extracted from wells there is dry steam, which is thought to have been stored as liquid in the rock pores and to have flashed to steam in the boreholes. Since 1968 reservoir pressure has declined from about 3.5 MPa to 2 MPa, while temperatures have remained constant at about 240° C in the main reservoir (Barker, et al., 1992; Barker and Pinogol, 1997; Mitchell Stark [Calpine Corp.], personal communication). In recent years, pressure decline has been mitigated by improved exploitation strategies, following concentration of production control in the hands of a single company (Goyal and Box, 2004).

Steam extraction and liquid injection at The Geysers induces continuous MEQ activity at a rate of several tens of events per day. They are widely distributed throughout the reservoir from the near surface to about 4-km depth (Eberhart-Phillips and Oppenheimer, 1984; Stark, 1992). They are monitored by a permanent network of more than 20 seismometers, 8 of which have three components. This is a good scenario for time-dependent MEQ tomography.

We inverted arrival times to obtain V_p and V_s using data sets of about 150 to 300 MEQs for each of the years 1991, 1993, 1994, 1996 and 1998 (Foulger, et al., 1997; Gunasekera, et al., 2003). In order to obtain the best possible result, we measured arrival times visually from digital seismograms using interactive MEQ processing software. We dealt with anisotropy by measuring shear-wave arrivals from numerically rotated horizontal-component seismograms (which enhance the clarity of the shear-wave arrival), and chose the earliest shear wave when there was evidence of shear-wave birefringence. The volume studied is 20 x 20 km in surface area (Fig. 1) and extends from -1 km above to 4 km below sea level. The tomographic images show significant differences in the structures for the different years. The full suite of results for V_p/V_s is shown in Figure 2.

The V_p/V_s structure at The Geysers for 1991 for sea level (upper panel) and 1 km below sea level (lower panel) is presented in Figure 2a. A strong negative anomaly of up to about 0.16 (9% below average) correlates closely with the most heavily exploited part of the steam reservoir. The difference between the 1991 anomaly and those for 1993, 1994, 1996 and 1998 are illustrated in Figures 2b-e. The anomaly grew steadily in strength between 1991 and 1998 in three parts of the reservoir. The largest change occurred in the center, with weaker changes to its SE and in a minor area to its NW, which first becomes detectable in 1998 when the time-interval has reached 7 years. The strength of the anomaly reached 13.4 percent below average during the seven-year study period.

The qualitative effects on V_p and V_s of processes expected to accompany geothermal production are shown schematically in Figure 3. The signs of the expected perturbations in wave speeds change if the processes are reversed, i.e., in the cases of replacement of steam by water, pressure increase and hydration of clay minerals. The magnitudes of the effects on V_p and V_s are

Figure 3 - Schematic diagram illustrating the expected effects of processes at producing geothermal fields. Large arrows indicate dominant effects and small arrows indicate subsidiary or small effects. The three processes have differing effects on V_p and V_s but all cause V_p/V_s to decrease. Drying: Water saturation has a large chemical-mechanical softening effect on argillaceous minerals such as illite, which are abundant at The Geysers. As pore fluid is removed and the minerals dry, V_p/V_s decreases because V_s increases ([Boitnott, 1995; Boitnott and Kirkpatrick, 1997) (adapted from Gunasekera et al., 2003).

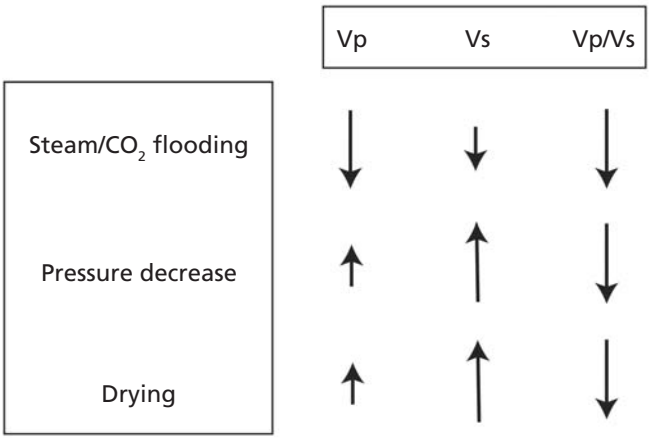

variable, but V_p/V_s decreases for steam flooding, pressure reduction, and dehydration of certain clay minerals. All these processes occur at The Geysers. As fluid is extracted, the liquid water in the pore space boils and is replaced by steam, increasing the macroscopic compressibility of the rocks and decreasing V_p. Reservoir pressure decreased greatly between 1991 and 1998, and the drying of argillaceous minerals such as illite caused an increase in the shear modulus of the rock matrix (Boitnott, 1995; Boitnott and Boyd, 1996), which caused V_s to increase. Thus, three effects serendipitously reinforced one another to cause a strong decrease in V_p/V_s with time.

Variations in the separate V_p and V_s fields indicate that the dominant process is water depletion in the center of the reservoir, and pressure reduction and mineral drying in the northwest and southeast regions. The rate at which V_p/V_s decreased between 1991 and 1998 suggests that most of the 1991 anomaly was caused by exploitation and thus the reservoir may have not been marked by a negative V_p/V_s anomaly in its natural state. It will be interesting to test this conclusion through study of reservoirs prior to exploitation.

Figure 4 - Map showing the 1989 seismic experiment at Mammoth Mountain, Long Valley caldera. The tomography grid used is outlined in black, with gridlines shown in gray. Circles: epicenters of MEQs used in tomography, black line: caldera ring fault, grey circle: resurgent dome, thin black lines: major faults. Mammoth Mountain and the Inyo Domes are shown in grey (adapted from Foulger et al., 2003).

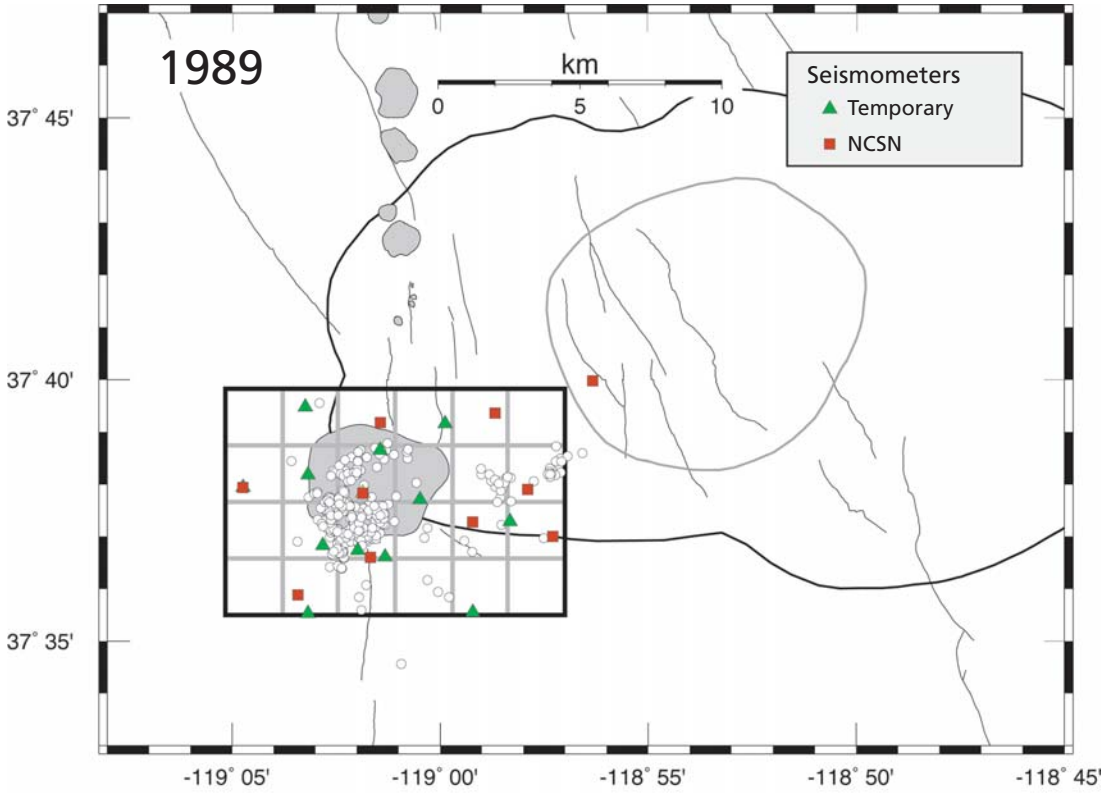

Mammoth Mountain, Long Valley Caldera, California

Long Valley Caldera is a silicic volcano in east-central California that has been experiencing seismic and volcanic unrest since 1978. Chronic, low-level activation of the magma system is associated with rapid ground deformation and earthquake activity. Mammoth Mountain, a 3,380-m dacite volcano on the southwest caldera rim, has been active since 1989 when an intense earthquake swarm accompanied the injection of a thin dike into the edifice (Hill, et al., 1990). This activity was accompanied by increased heat flow, venting of CO_2, and temporal changes in $^3He/^4He$ ratios in a steam vent on the mountain. Sustained and widespread diffuse venting of CO_2 through the soil has occurred subsequently, killing large areas of trees. The total flux has been estimated to be 200 to 500 tonnes/day (Farrar, et al., 1995; Gerlach, et al., 1999), although this rate has decreased with time.

Sorey, et al. [1998] propose that the upper 2 km of Mammoth Mountain is relatively cold and dry and underlain by a 150°C, high-pressure CO_2 gas pocket that may occupy several tens of cubic kilometers of porous and/or highly fractured rock. The pocket is capped by an impermeable rock unit, and perhaps underlain by a CO_2-saturated liquid water reservoir. The cap may have ruptured in the 1989 seismo-volcanic crisis, allowing gas to leak out at a high rate. The total amount of gas emitted from 1989 to 1997 is equivalent to the total degassing of <1.0 km3 of CO_2-saturated rock with a porosity of 0.01 at pressures corresponding to the inferred depth of the pocket (Sorey, et al., 1998).

Dense three-component digital seismic networks were operated at Mammoth Mountain during the 1989 crisis and again in 1997. In 1997, several of the sites used in 1989 were reoccupied, to minimize systematic errors arising from variations in network geometry (Fig. 4). In both experiments, enough earthquakes occurred beneath Mammoth Mountain to enable tomographic inversions for V_p and V_p/V_s throughout about the upper 5 km (Foulger, et al., 2003).

Inversion of the 1989 data revealed a coherent negative V_p/V_s anomaly in the upper 2 - 3 km beneath Mammoth Mountain, with a maximum strength of 9 percent. The edge of this anomaly correlates closely with areas of surface CO_2 venting, which led Julian, et al. (1998) to interpret it as the ruptured CO2 reservoir.

The amount of CO_2 lost from beneath Mammoth Mountain from 1989 to 1997 is small compared with the amount of fluid extracted from The Geysers, and thus much weaker wave-speed changes are expected. Both increases and decreases in V_p and V_s of up to a few percent occurred in different places beneath the volcano, as is consistent with variable redistribution of pore water and CO_2. The change in the V_p/V_s field shows, however, a coherent increase throughout a zone that girdles the southern half of Mammoth Mountain (Fig. 5). The whole zone correlates with areas that experienced significant CO_2 degassing. In particular the areas of V_p/V_s increase beneath the southwest and south sides of Mammoth Mountain directly underlie the Reds Creek and Horseshoe Lake tree-kill areas, which have been estimated to vent over four times as much as all the other tree-kill areas combined (Sorey, et al., 1998).

Theoretical relations and laboratory measurements of seismic wave speeds in sandstones saturated with hydrocarbon and CO_2 (Wang and Nur, 1989) show that V_p/V_s decreases significantly with CO_2 flooding because of an increase in bulk compressibility (Fig. 3). However, a recent study in the McElroy oil field, Texas, showed that flooding the oil reservoir *in situ* with CO_2 produced a pore pressure increase that offset the increase in compressibility of the bulk rock that resulted from CO_2 flooding (Wang and Nur, 1989). Thus the V_p/V_s ratio might remain

Figure 5 - V_p/V_s structure determined from tomography at three depths for the Mammoth Mountain area (small box, Fig. 4). Left panels: model for 1989; middle panels: model for 1997; right panels: difference between the 1997 and 1989 models. Blue symbols: CO2-rich springs. Areas of tree kill caused by surface CO_2 venting are shown in white (adapted from Foulger et al., 2003).

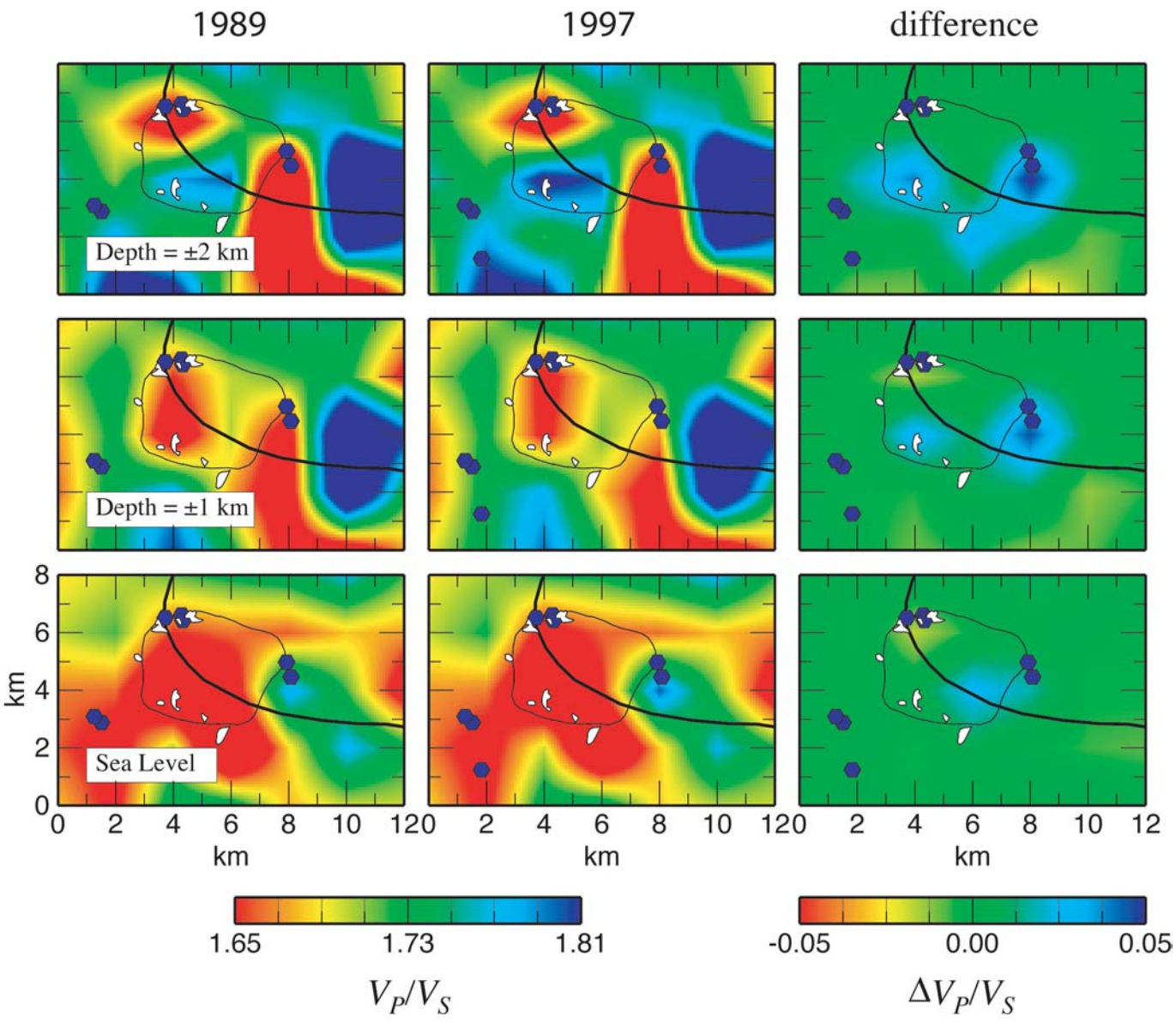

unchanged. The McElroy oil field is a reasonable analog of the shallow levels beneath Mammoth Mountain. The CO_2 flooding occurred at a depth of 900 m below the surface, where the reservoir rock is composed of dolostones and evaporite cement. The porosity and permeability average 10% and 0.01 - 90 x 10^{-11} cm^2 respectively. At the time of CO_2 flooding, the pore fluid in the McElroy field was half water and half oil, with a density of 0.85 g cm^{-3} at 16°C and 1 atmospheric pressure.

Examination of the separate changes in V_p and V_s suggest that between 1990 and 1997, gas migrated into a volume in roughly the top 2 km beneath the center of Mammoth Mountain approximately overlying the dike or crack that opened in 1989, and was depleted in peripheral volumes that correlate with surface venting areas. The source of the CO_2 is most likely the gas pocket underneath.

The seismic network deployed in 1997 also encompassed the Casa Diablo Hot Springs geothermal area on the southwest edge of the Long Valley resurgent dome. We found a small negative V_p/V_s anomaly adjacent to this geothermal area, extending through the upper ~2 km. This observation is most readily explained by an increase in vapor content in a localized volume of about 8 km^3. The tomographic results provide no evidence of elevated temperatures beneath Casa Diablo Hot Springs, in agreement with evidence from drilling and prospecting, that suggests the area is not a primary zone of upwelling where temperature increases with depth. The Casa Diablo anomaly is probably caused by a highly fractured, geothermal fluid containment volume (Foulger et al., 2003). These results provide a useful baseline measure of V_p/V_s structure against which future images may be compared.

Coso Geothermal Area, California

Time-dependent tomography following a similar procedure is currently underway at the producing Coso geothermal area (Foulger and Julian, 2004). The objectives are both to monitor long-term evolution of the reservoir and to test the method for its ability to monitor reservoir stimulation experiments involving fluid injection, conducted as part of an ongoing U.S. Department of Energy Enhanced Geothermal Systems project at Coso (Rose, et al., 2003).

Since the early 1990s, a network of 18 three-component digital borehole seismometers operated by the U. S. Navy has monitored microearthquakes at Coso. Thirteen of these seismometers lie within or near the producing steam field (Fig. 6). The Coso geothermal area is highly active seismically, typically producing 10 to 15 earthquakes per day, well distributed throughout the area. It is thus well suited for time-dependent tomography.

Figure 6 - Map showing the location of the area at the Coso geothermal area studied using tomography.

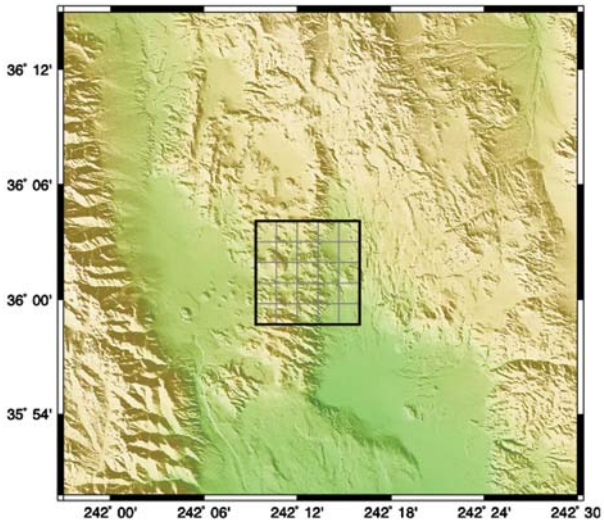

Preliminary results show detectable wave-speed changes between 1996 and 2002 (Foulger and Julian, 2004). Inversion of the 1996 data reveals a negative V_p/V_s anomaly in the upper ~2 km in the north-central part of the area, which correlates closely with the most productive part of the geothermal reservoir. Negative V_p and V_s anomalies in the northwest and northeast coincide approximately with high V_p/V_s values at depths of 1- to 2-km below the surface. Such correlation is unusual and was not observed either at The Geysers or Mammoth Mountain.

Comparing the structures for 1996 and 2002 shows that during the interim period, both V_p and V_s increased, but increases in V_s dominated (Fig. 7), so the negative V_p/V_s anomaly became stronger. The changes observed are consistent with the replacement of pore liquid with steam at shallow depth, pressure decrease, or the dehydration of some minerals. When completed, the study of the Coso Geothermal Field may comprise the most valuable case history to date for this method, since the tomographic results are of high quality and all the reservoir data are held by a single operator.

Future Challenges

To increase the utility of this promising method, developments along three main lines are needed. First, additional case histories are required. The results of several studies, e.g., in Indonesian geothermal fields, have not been published for reasons of propriety. Releasing these results would be a useful service to the geothermal community.

Second, software custom-designed for application to geothermal targets is needed. At present, only software intended for general tectonic targets of local-to-regional areal extent is available. A useful improvement on the method currently used would be the development of a program optimized for targets with spatial dimensions of a few kilometers and able to invert datasets from two or more epochs simultaneously. At present, datasets are inverted independently and the results subsequently differenced, an approach that makes estimating confidence levels difficult. The subtle signals being sought require the best numerical methods possible.

Third, tomographic results must be compared with production data and other information bearing on the physical evolution of reservoirs so that the changes in V_p, V_s and V_p/V_s may be understood quantitatively. When this is achieved, time-dependent MEQ tomography will provide a powerful tool to quantify the depletion of geothermal reservoirs and guide injection strategies to maximize their lifetimes.

Figure 7 - Preliminary results from tomography at the Coso geothermal area, showing V_p/V_s structure 1 km above sea level. Left panel: model for 1996; middle panel: model for 2002; right panel: difference between 2002 and 1996. The scale at left applies to the left and middle panels, and the scale at right applies to the right panel. Notice differences in sensitivities of the scales.

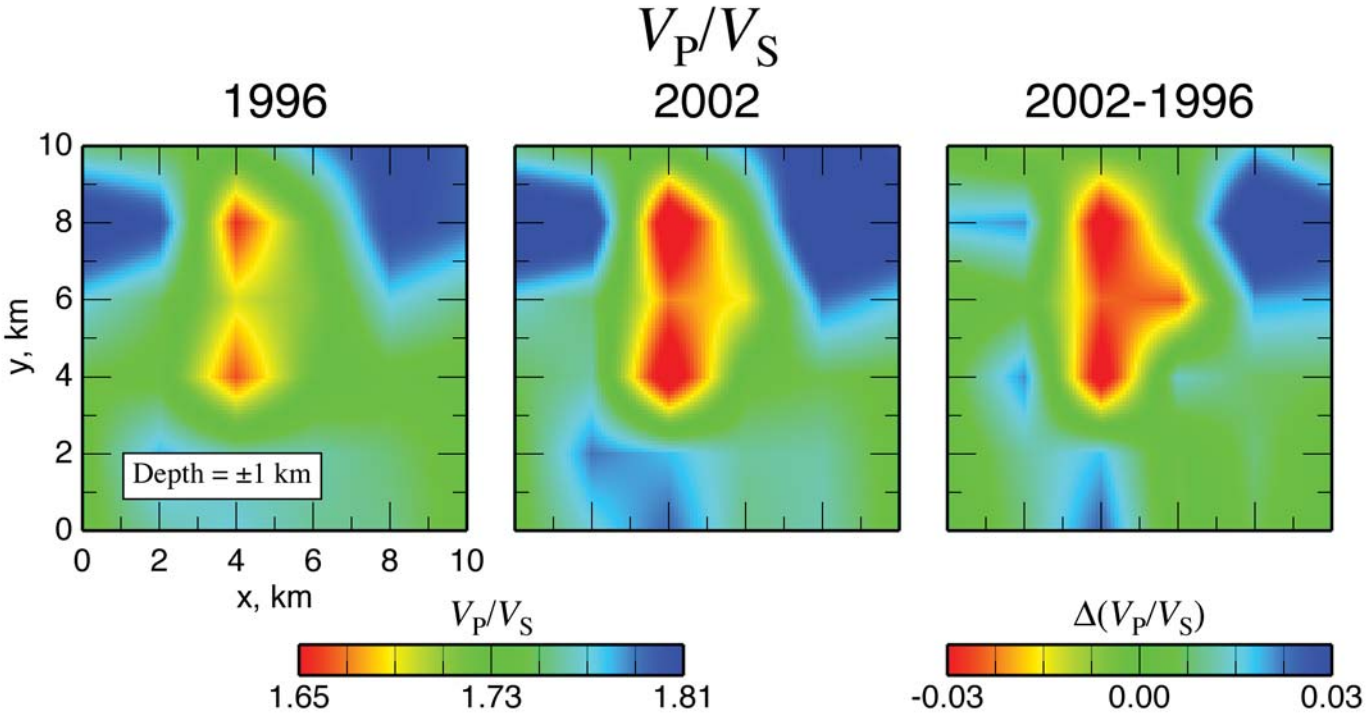

Acknowledgments

Numerous individuals contributed to this work over the years. We particularly thank UNOCAL Corp., the U.S. Navy and the University of Utah for assistance in obtaining data and for many helpful discussions. This work was supported by NERC Grant GR9/134, a DENI Ph.D. scholarship, NERC M.Sc. scholarships, equipment loans from the NERC (loan 540/0197) and IRIS-PASSCAL, the U.S. Forest Service and the Mono County government. ■

References

Barker, B.J., M.S. Gulati, M.A. Bryan, and K.L. Riedel, 1992. "Geysers Reservoir Performance," Geothermal Resources Council *Monograph on The Geysers Geothermal Field*, edited by C. Stone, pp. 167-177.

Barker, B.J., and A.S. Pinogol, 1997. "Geysers Reservoir Performance - An Update," *Proceedings*, Stanford University 22nd Workshop on Geothermal Reservoir Engineering.

Boitnott, G.N., 1995. "Laboratory Measurements on Reservoir Rocks from The Geysers Geothermal Field," *Proceedings*, Stanford University 20th Workshop on Geothermal Reservoir Engineering, pp. 107-114.

Boitnott, G.N., and P.J. Boyd, 1996. "Permeability, Electrical Impedance, and Acoustic Velocities on Reservoir Rocks from The Geysers Geothermal Field," *Proceedings*, 21st Workshop on Geothermal Reservoir Engineering, pp. 343-350.

Boitnott, G.N., and A. Kirkpatrick, 1997. "Interpretation of Field Seismic Tomography at The Geysers Geothermal Field, California," *Proceedings*, Stanford University 22nd Workshop on Geothermal Reservoir Engineering.

Eberhart-Phillips, D., 1986. "Three-Dimensional Velocity Structure in the Northern California Coast Ranges from Inversion of Local Earthquake Arrival Times," *Bulletin of the Seismological Society of America*, vol. 76, pp. 1025-1052.

Eberhart-Phillips, D., and D.H. Oppenheimer, 1984. "Induced Seismicity in The Geysers Geothermal Area, California, *Journal of Geophysical Research*, vol. 89, pp. 1191-1207.

Evans, J.R., D. Eberhart-Phillips, and C.H. Thurber, 1994. *User's Manual for SIMULPS12 for Imaging VP and VP/VS, A Derivative of the Thurber Tomographic Inversion SIMUL3 for Local Earthquakes and Explosions*, U.S. Geological Survey Open File Report, pp. 142.

Farrar, C.D., M.L. Sorey, W.C. Evans, J.F. Howle, B.D. Kerr, B.M. Kennedy, C.Y. King, and J.R. Southon, 1995. "Forest-Killing Diffuse CO2 Emission at Mammoth Mountain as a Sign of Magmatic Unrest," *Nature*, vol. 376, pp. 675-678.

Foulger, G.R., C.C. Grant, A. Ross, and B.R. Julian,1997. "Industrially Induced Changes in Earth Structure at The Geysers Geothermal Area, California, *Geophysical Research Letters*, vol. 24, pp. 135-137.

Foulger, G.R., and B.R. Julian, 2004. "Changes in Three-Dimensional Seismic Structure 1996 - 2002 at the Coso Geothermal Area, California: A Possible Monitoring Tool for Engineered Geothermal Systems," *Proceedings*, Stanford University 29thWorkshop on Geothermal Reservoir Engineering.

Foulger, G.R., B.R. Julian, A.M. Pitt, D.P. Hill, P. Malin, and E. Shalev, 2003. "Tomographic Crustal Structure of Long Valley Caldera, California, and Evidence for the Migration of CO2 Between 1989 and 1997," *Journal of Geophysical Research*, vol. 108.

Foulger, G.R., A.M. Pitt, B.R. Julian, and D.P. Hill, 1995. "Three-Dimensional Structure of Mammoth Mountain, Long Valley Caldera, from Seismic Tomography, *EOS Transactions*, American Geophysical Union, vol. 76 (Fall Meeting Supplement).

Gerlach, T.M., M.P. Doukas, K.A. McGee, and R. Kessler, 1999. "Airborne Detection of Diffuse Carbon Dioxide Emissions at Mammoth Mountain, California, *Geophysical Research Letters*, vol. 26, pp. 3661-3664.

Goyal, K.P., and W.T. Box, 2004. "Geysers Performance Update Through 2002" (Abstract), *Proceedings*, Stanford University 29th Workshop on Geothermal Reservoir Engineering.

Gunasekera, R.C., G.R. Foulger, and B.R. Julian, 2003. "Four Dimensional Tomography Shows Progressive Pore-Fluid Depletion at The Geysers Geothermal Area, California, *Journal of Geophysical Research*, vol. 108.

Hill, D.P., W.L. Ellsworth, M.J.S. Johnston, J.O. Langbein, D.H. Oppenheimer, A.M. Pitt, P.A. Reasenberg, M.L. Sorey, and S.R. McNutt, 1990. "The 1989 Earthquake Swarm Beneath Mammoth Mountain, California: An Initial Look at the 4 May through 30 September Activity," *Bulletin of the Seismological Society of America*, vol. 80, pp. 325-339.

Julian, B.R., A.M. Pitt, and G.R. Foulger, 1998. "Seismic Image of a CO2 Reservoir Beneath a Seismically Active Volcano," *Geophysical Journal International*, vol. 133, pp. 7-10.

Rose, P.E., C. Barton, J. McCulloch, J.M. Moore, K. Kovac, J. Sheridan, P. Spielman, and B. Berard, 2003. "The Coso EGS Project - Recent Developments," Geothermal Resources Council *Transactions*, vol. 27, pp. 879-883.

Sorey, M.L., W.C. Evans, B.M. Kennedy, C.D. Farrar, L.J. Hainsworth, and B. Hausback, 1998. "Carbon Dioxide and Helium Emissions from a Reservoir of Magmatic Gas Beneath Mammoth Mountain, California," *Journal of Geophysical Research*, vol. 103, pp. 15,303-15,323.

Stark, M.A., 1992. "Microearthquakes - A Tool to Track Injected Water in The Geysers Reservoir," *Monograph on The Geysers Geothermal Field*, C. Stone, Ed., pp. 111-120, Geothermal Resources Council, Davis, CA.

Thurber, C.H., 1981. *Earth Structure and Earthquake Locations in the Coyote Lake Area, Central California*, Ph.D. thesis, Massachusetts Institute of Technology, Cambridge, MA.

Wang, Z., and A.M. Nur, 1989. "Effects of CO2 Flooding on Wave Velocities in Rocks with Hydrocarbons," *Society of Petroleum Engineers*, vol. 3, pp. 429-436.